Organic Process Research & Development **2009**, *13*, 1007–1013

Microreactor-Based Synthesis of Molecularly Imprinted Polymer Beads Used for Explosive Detection

Dirk Roeseling,* Tobias Tuercke, Horst Krause, and Stefan Loebbecke

Fraunhofer Institute for Chemical Technology (ICT), Joseph-von-Fraunhofer-Strasse 7, 76327 Pfinztal, Germany

Abstract:

Molecularly imprinted polymer (MIP) beads based on acrylate formulations have been successfully synthesized in two different types of microreactors capable of generating spherical prepolymer droplets of controlled size in continuous segmented flow processes. After polymerizing and curing the droplets monodisperse acrylate particles have been obtained. Particle sizes have been adjusted in a wide range from 10 to 140 μm by choosing appropriate flow rates of the continuous and the disperse phase. By adding trinitrotoluene (TNT) as a template and PEG as a coporogen to the disperse phase MIP beads with TNT-selective sites and a sufficiently high porosity have been synthesized, as required, for explosive detection techniques.

Introduction

For several years, microstructured reactors have been enjoying a successful advance into chemical laboratories. Global research activities have clearly demonstrated that the application of microstructured reactors, mixers, and other microfluidic components offers numerous technical advantages for chemical processes such as improved heat and mass transfer as well as short residence times, which can be precisely adjusted.[1−3]

Segmented Flow Processes. Microstructured reactors can also be used to process multiphase fluid systems (e.g., liquid/liquid or gas/liquid) with high precision in the form of segmented flows—which opens up new opportunities for interesting applications. In specially developed microfluidic structures, fluids can be continuously segmented into a second liquid phase by shearing them off or constricting them in the form of droplets or bubbles. The size of the droplets or bubbles formed and the frequency of segmentation can be controlled very precisely through the selected flow conditions, reactor geometries, and other process parameters.[4−7]

Segmented flow processing in microfluidic reactors can be used to deliberately intensify the interaction between two-phase systems. By providing large interfacial areas, the mass transport over the phase boundary layers can be significantly accelerated compared to macroscopic processes. Typical applications are phase transfer catalytic reactions and other two-phase organic syntheses.[8−10]

On the other hand, the droplets or fluid segments formed can also be used as closed reaction vessels having no chemical interaction with the transport phase. Within the fluid segments (each with a volume of just a few nanoliters) syntheses of fine chemical products can be performed by suppressing cross-contamination and dilution and dispersion effects caused by convection and diffusion. Moreover, mixing of the reagents in the nanoliter segment is strongly intensified by advection.[5] Droplet reactors have been also used for the synthesis of multiple emulsions[11,12] and nanoparticles.[13−15]

More recently, microfluidic segmented flow processes have been used for polymerization reactions, providing a novel route to preparing monodisperse polymer particles of highly controlled size and shape.[16−19]

Here, we report on the synthesis of uniform molecularly imprinted polymer (MIP) beads which were successfully prepared in different types of microfluidic reactors.

Molecularly Imprinted Polymers (MIPs). MIPs have received increasing interest in the field of extraction, enantiomer separation, product isolation, or enrichment of species from diluted samples as the polymers can be tailored with a high selectivity for a predetermined ligand or analyte.[20−22] A quite new field is the use of MIPs for the detection of organic compounds and especially of explosives such as trinitrotoluene

* Corresponding author. E-mail: dirk.roeseling@ict.fraunhofer.de.

(1) Jaehnisch, K.; Hessel, V.; Loewe, H.; Baerns, M. *Angew. Chem., Int. Ed.* **2004**, *43*, 406–446.
(2) Kockmann, N.; Gottsponer, M.; Zimmermann, B.; Roberge, D. M. *Chem.—Eur. J.* **2008**, *14*, 7470–7477.
(3) Watts, P.; Wiles, C. *Chem. Commun.* **2007**, 443–467.
(4) Kreutzer, M. T.; Kapteijn, F.; Moulijn, J. A.; Heiszwolf, J. J. *Chem. Eng. Sci.* **2005**, *60*, 5895–5916.
(5) Song, H.; Chen, D. L.; Ismagilov, R. F. *Angew. Chem., Int. Ed.* **2006**, *45*, 7336–7356.
(6) The, S.-Y.; Lin, R.; Hung, L.-H.; Lee, A. P. *Lab Chip* **2008**, *8*, 198–220.
(7) Huebner, A.; Sharma, S.; Srisa-Art, M.; Hollfelder, F.; Edel, J. B.; deMello, A. J. *Lab Chip* **2008**, *8*, 1244–1254.
(8) Ueno, M.; Hisamoto, H.; Kitamori, T.; Kobayashi, S. *Chem. Commun.* **2003**, 936–937.
(9) Dummann, G.; Quittmann, U.; Groeschel, L.; Agar, D. W.; Woerz, O.; Morgenschweis, K. *Catal. Today* **2003**, *79−80*, 433–439.
(10) Okamoto, H. *Chem. Eng. Technol.* **2006**, *29*, 504–506.
(11) Chu, L.-Y.; Utada, A. S.; Shah, R. K.; Kim, J.-W.; Weitz, D. A. *Angew. Chem.* **2007**, *119*, 9128–9132.
(12) Nisisako, T. *Chem. Eng. Technol.* **2008**, *31*, 1091–1098.
(13) Xu, S.; Nie, Z.; Seo, M.; Lewis, P.; Kumacheva, E.; Stone, H. A.; Garstecki, P.; Weibel, D. B.; Gitlin, I.; Whitesides, G. M. *Angew. Chem.* **2005**, *117*, 734–738.
(14) Sotowa, K.-I.; Irie, K.; Fukumori, T.; Kusakabe, K.; Sugiyama, S. *Chem. Eng. Technol.* **2007**, *30*, 383–388.
(15) Frenz, L.; El Harrak, A.; Pauly, M.; Bégin-Colin, S.; Griffiths, A. D.; Baret, J.-C. *Angew. Chem., Int. Ed.* **2008**, *47*, 6817–6820.
(16) Nisisako, T.; Torii, T.; Higushi, T. *Chem. Eng. J.* **2004**, *101*, 23–29.
(17) Serra, C. A.; Chang, Z. *Chem. Eng. Technol.* **2008**, *31*, 1099–1115.
(18) Gross, G. A.; Hamann, C.; Guenther, M.; Koehler, J. M. *Chem. Eng. Technol.* **2007**, *30*, 341–346.
(19) Bouquey, M.; Serra, C.; Berton, N.; Prat, L.; Hadziioannou, G. *Chem. Eng. J.* **2008**, *135* (1), S93–S98.
(20) Wulff, G.; Sarhan, A. *Angew. Chem.* **1972**, *84*, 364.
(21) Sellergren B., Ed. *Molecularly Imprinted Polymers: Man-made Mimics of Antibodies and their Applications in Analytical Chemistry*; Elsevier Science B. V.: Amsterdam, 2001.
(22) Tokonami, S.; Shiigi, H.; Nagaoka, T. *Anal. Chim. Acta* **2009**, *641*, 7–13.

10.1021/op9001774 CCC: $40.75
Published on Web 09/18/2009

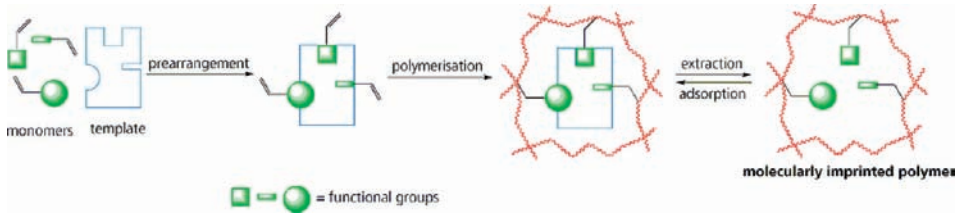

Figure 1. **Principal procedure for the synthesis of MIPs.**

(TNT), dinitrotoluene (DNT), and dinitrodimethylbutane (DMNB).[23,24] Sensor networks based on MIP technology can be used as monitoring systems for the surveillance of complex areas. The synthesis of MIPs is usually carried out by suspension polymerization in batch processes in the presence of a template. Subsequent removal of the template by extraction or other techniques reveals "imprinted" binding sites that are specific towards the analyte (here: traces of explosives) via either covalent or noncovalent interactions. Figure 1 illustrates schematically the principal procedure of a MIP synthesis. For applications such as chromatography, extraction, or analyte enrichment small MIP particles are required that can be packed into columns or cartridges. Usually, the polymer particles obtained from batchwise suspension polymerization show a broad particle size distribution, and larger particles have to be crushed and ground to smaller sizes.

To achieve both a more constant performance of the imprinted polymer particles and superior flow characteristics in the packed column, MIP beads of spherical shape with a narrow particle size distribution are highly required. Unfortunately, methods described so far for preparing uniform spherical MIPs are either using expensive solvents and monomers or employing complex shape polymerization techniques.[25,26] An alternative approach is the application of segmented flow processes in microreactors as recently proposed by Zourob et al.[27] In our work, we have refined this approach to obtain monodisperse spherical MIP particles based on acrylate polymers with highly functionalized inner surfaces. For this purpose, we have transferred the two-phase suspension polymerization batch process to a continuous two-phase microreaction process.

Experimental Section

General Procedure. Similar to the classical batch process, oil-in-water emulsions were generated in the microfluidic segmented flow process. Water was used as continuous phase, and an acrylate-based formulation (containing a functional acrylate monomer, a cross-linking agent, a porogen, and a photosensitive initiator) was used as disperse phase. The acrylate droplets that were continuously formed in the microreactor were cured by UV radiation once they leave the microfluidic structure.

In order to create a temporary stable emulsion until the droplets were cured, a nonionic surfactant was added to the continuous phase, preventing coalescence and diffusion instability caused by Ostwald ripening. The latter occurs even if the disperse phase (acrylate) is only slightly soluble in the continuous phase (water). As a consequence, the acrylate diffuses from the smaller droplets across the aqueous phase towards larger droplets. The net effect is a reduction in total interfacial area, and consequently in interfacial energy. When the droplet diameter has reached a critical lower limit the droplet disappears ("Kelvin instability"). Therefore, we have stabilized the interfacial surface by adding 4% of polyvinyl alcohol (PVA) to the continuous phase.

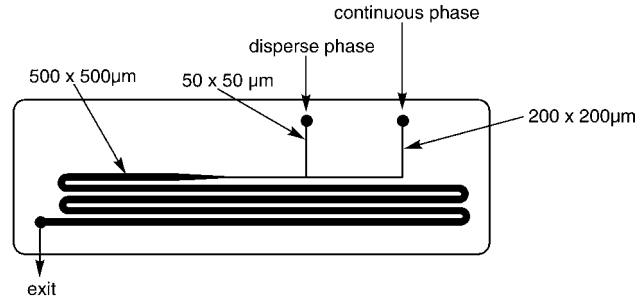

Figure 2. **T-junction microreactor.**

To achieve good sensing properties, MIP particles have to provide a large inner surface with active sites which are easily accessible by the analyte. Therefore, it is essential that an appropriate porogen is incorporated into the acrylate formulation. In classical suspension or emulsion polymerizations used for MIP synthesis organic solvents such as chloroform, dimethylformamide, or acetonitrile are used for this purpose. In this work, however, we have added different amounts of polyethylene glycol, a soluble polymeric Thermoplast used as a coporogen, to the disperse phase.

Microreactors and Setup. The segmentation and droplet formation were investigated in two different types of microreactors, a T-junction microreactor and a flow-focussing microreactor, both made of glass.

In the segmentation area of the T-junction microreactor two rectangular microchannels of different channel sizes join (Figure 2). The microchannel for the continuous phase is 200 μm wide and 200 μm deep whereas the cross-section dimension of the disperse phase microchannel is 50 μm × 50 μm. Once the segmented flow is formed, it passes through an enlarged residence time channel (500 μm × 500 μm) of approximately 17 cm length.

In the flow-focussing device (Figure 3) the disperse phase is introduced via a single microchannel (200 μm × 200 μm) whereas the continuous phase is introduced simultaneously via two inlet channels of similar size. The continuous phase thus surrounds the disperse phase and finally constricts it, forming droplets. The so-formed segmented flow is released into a

(23) Dickert, F. L.; Hayden, O. *Trends Anal. Chem.* **1999**, *18*, 192–199.
(24) Bunte, G.; Hürttlen, J.; Pontius, H.; Hartlieb, K.; Krause, H. *Anal. Chim. Acta* **2007**, *591*, 49–56.
(25) Mayes, A. G.; Mosbach, K. *Anal. Chem.* **1996**, *68*, 3769–3774.
(26) Chen, Z.; Zhao, R.; Shangguan, D.; Liu, G. *Biomed. Chromatogr.* **2005**, *19*, 533–538.
(27) Zourob, M.; Mohr, S.; Mayes, A. G.; Macaskill, A.; Pérez-Moral, N.; Fielden, P. R.; Goddard, N. J. *Lab Chip* **2006**, *6*, 296–301.

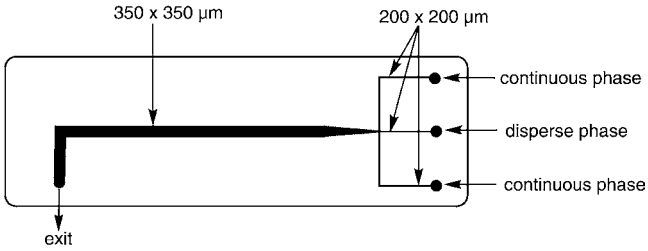

Figure 3. **Flow-focussing microreactor.**

residence time channel (350 μm × 350 μm) of approximately 6 cm length.

All fluids were pumped by pulsation-free syringe pumps to ensure even droplet formation and precise variation of flow rates and flow rate ratios. For the continuous phase an Isco Series D 500 pump (Isco Inc., U.S.A.) was used, whereas the disperse phase was pumped by a Harvard PHD4400 syringe pump (Harvard Apparatus Ltd., U.K.).

The prepolymer droplets formed in the microreactors were collected in a beaker containing 10 mL of the continuous phase stirred at 250 rpm. Photocuring of the droplets was performed for 30 min at room temperature by employing a Bluewave 50 UV source (Dymax GmbH, Germany) which was submerged into the beaker. After completion of curing, the polymer beads formed were characterized by measuring the mean particle size and size distribution (Malvern Mastersizer S, Malvern Instruments Ltd., U.K.) and their inner surfaces by employing a BET Analyzer based on nitrogen absorption (Quantachrome Nova 2000e, Quantachrome GmbH, Germany).

Formulations and Materials. A 4% solution of polyvinyl alcohol (PVA 4-88, Merck) in water was used as continuous phase.

The basic formulation of the dispersed phase for nonimprinted polymers consisted of 20 mL of chloroform (puriss., Roth), 1.38 g (0.016 mol) of methacrylic acid (MAA, Aldrich), 19.82 g (0.1 mol) of ethylene glycol dimethacrylate (EGDMA, Fluka), and 0.6 g (0.0014 mol) of Irgacure 819 (Ciba Speciality Chemicals). All acrylates used were freshly distilled to remove stabilisers.

In case of synthesizing imprinted polymer beads, 900 mg (0.0039 mol) of trinitrotoluene (TNT, recrystallized from in-house resources) was added as a template. To enlarge the inner surface and thus enhance the porosity of the resulting polymer beads, different amounts of polyethylene glycol (PEG, MW 32000, Aldrich) were added to the disperse phase.

Results and Discussion

T-Junction Microreactor. Two sets of experiments were carried out with the T-junction microreactor using the basic formulation with TNT as a template for the synthesis of imprinted polymer beads (MIP) and without any template for the synthesis of nonimprinted polymer beads (NIP). In all experiments, the flow rate of the continuous phase Q_C was kept constant at 0.4 mL/min, whereas the flow rate of the disperse phase Q_D was varied between 0.001 to 0.008 mL/min. As the maximum pressure drop within the T-junction microreactor was limited to 5 bar, no higher Q_C flow rates were applied. Consequently, the maximum turnover of the reactor was restricted to 0.5 g of polymer particles per hour.

Table 1. **Polymer beads synthesized in the T-junction microreactor at Q_C = 0.4 mL/min**

nonimprinted polymer	Q_C/ (mL/min)	Q_D/ (mL/min)	Q_C/Q_D	mean particle size/μm	span (84/16)
run 1	0.4	0.008	50	43.50	0.153
run 2	0.4	0.004	100	36.94	0.152
run 3	0.4	0.002	200	28.36	0.201
run 4	0.4	0.001	400	11.80	0.198
imprinted polymer	**Q_C/ (mL/min)**	**Q_D/ (mL/min)**	**Q_C/Q_D**	**mean particle size/μm**	**span (84/16)**
run 1	0.4	0.008	50	42.17	0.271
run 2	0.4	0.004	100	36.56	0.254
run 3	0.4	0.002	200	25.68	0.181
run 4	0.4	0.001	400	10.91	0.194

In Table 1 the mean particle size and the particle size distribution of all synthesized polymer beads are summarized. The particle size distribution is indicated by dimensionless span values derived from a volume weighted particle size model. The span (84/16) value is defined as:

$$\text{span}(84/16) = (d_{84\%} - d_{16\%})/d_{50\%} \qquad (1)$$

Span(84/16) values of 0.2 and below are indicating a monodisperse particle size distribution.

Table 1 clearly shows that the mean particle size of both MIP and NIP beads could be deliberately varied in a range between approximately 10 and 45 μm by changing the Q_C/Q_D flow rate ratio. Figure 4 shows a nearly linear behavior within this particle size range. The corresponding span(84/16) values indicate that in most experiments a monodisperse particle size distribution was obtained. MIP beads tend to appear with a slightly broader particle size distribution compared with NIP beads since the template can hinder the curing process to a certain extent.

Flow-Focussing Microreactor. To investigate droplet formation and polymer bead synthesis at higher flow rates and thus to enhance the turnover of the segmented flow process further, experiments were carried out by employing the flow-focussing microreactor.

In a first series of experiments MIP and NIP particles were synthesized at a 5 times higher flow rate of the continuous phase (Q_C = 2.0 mL/min). The flow rate of the disperse phase was also increased and varied in the range of 0.005−0.100 mL/min. However, the flow rate ratio Q_C/Q_D was similar to the experiments conducted in the T-junction microreactor. Again,

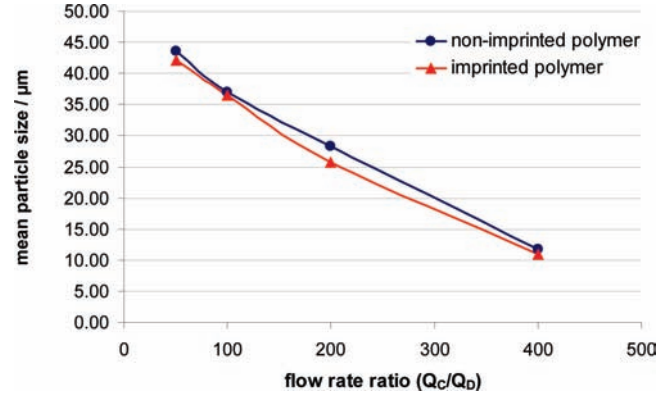

Figure 4. **Mean particle sizes of polymer beads synthesized in the T-junction microreactor at different flow rate ratios.**

Table 2. **Polymer beads synthesized in the flow-focussing microreactor at Q_C = 2.0 mL/min**

nonimprinted polymer	Q_C/ (mL/min)	Q_D/ (mL/min)	Q_C/Q_D	mean particle size/μm	span (84/16)
run 1	2.0	0.100	20	140.32	0.115
run 2	2.0	0.050	40	88.39	0.176
run 3	2.0	0.025	80	51.05	0.233
run 4	2.0	0.010	200	21.55	0.357
run 5	2.0	0.005	400	17.16	0.311
nonimprinted polymer	Q_C/ (mL/min)	Q_D/ (mL/min)	Q_C/Q_D	mean particle size/μm	span (84/16)
run 1	2.0	0.100	20	139.96	0.165
run 2	2.0	0.050	40	75.61	0.256
run 3	2.0	0.025	80	47.80	0.247
run 4	2.0	0.010	200	27.20	0.231
run 5	2.0	0.005	400	22.54	0.193

the mean particle size of both MIP and NIP beads could be deliberately changed from approximately 20 to 140 μm by changing the flow rate ratio Q_C/Q_D from 400 to 20 (Table 2). Figure 5 shows the exponential decrease of the mean particle size when Q_C/Q_D is increased. Span(84/16) values between 0.115 and 0.357 indicate that either monodisperse or almost monodisperse particles were obtained. As an example, Figure 6 shows a light microscope picture of 20 μm droplets generated in the flow-focussing microreactor (Q_C: 2.0 mL/min; Q_D: 0.005 mL/min) which confirms the spherical shape and monodisperse droplet size.

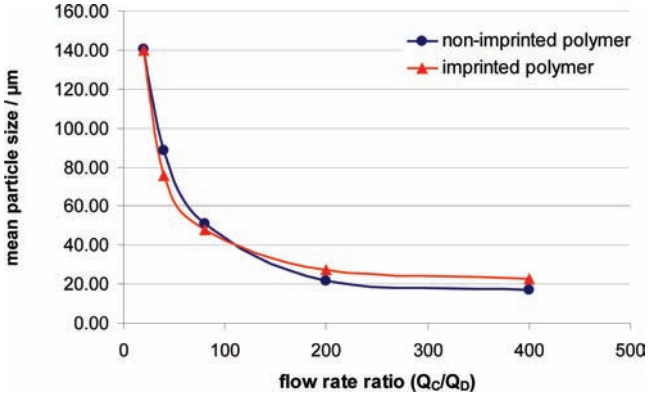

Figure 5. **Mean particle sizes of polymer beads synthesized in the flow-focussing microreactor at different flow rate ratios but at a fixed flow rate of the continuous phase (Q_C = 2.0 mL/min).**

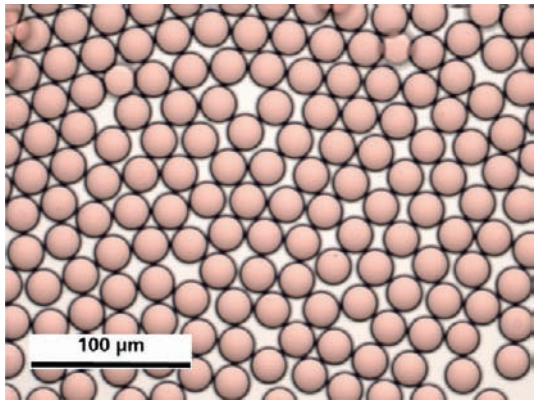

Figure 6. **Light microscope picture of monodisperse polymer droplets (size: 20 μm) formed within the flow-focussing microreactor (Q_C = 2.0 mL/min; Q_D = 0.005 mL/min).**

Table 3. **Polymer beads synthesized in the flow-focussing microreactor at elevated flow rates of the continuous phase**

nonimprinted polymer	Q_C/ (mL/min)	Q_D/ (mL/min)	Q_C/Q_D	mean particle size/μm	span (84/16)
run 1	2.0	0.100	20	140.32	0.115
run 2	2.0	0.050	40	88.39	0.176
run 3	2.0	0.025	80	51.05	0.233
run 4	2.0	0.010	200	21.55	0.357
run 5	2.0	0.005	400	17.16	0.311
run 1	4.0	0.200	20	132.98	0.266
run 2	4.0	0.100	40	72.21	0.469
run 3	4.0	0.050	80	57.58	0.205
run 4	4.0	0.020	200	24.94	0.211
run 5	4.0	0.010	400	16.83	0.261
run 1	6.0	0.300	20	55.84	0.536
run 2	6.0	0.150	40	50.60	0.502
run 3	6.0	0.075	80	44.17	0.654
run 4	6.0	0.030	200	39.75	0.561
run 5	6.0	0.015	400	36.44	0.302
run 1	8.0	0.400	20	32.80	0.434
run 2	8.0	0.200	40	23.44	0.516
run 3	8.0	0.100	80	26.49	0.469
run 4	8.0	0.040	200	23.80	0.397
run 5	8.0	0.020	400	15.07	0.406
run 1	10.0	0.500	20	30.26	0.671
run 2	10.0	0.250	40	42.93	0.568
run 3	10.0	0.125	80	47.77	0.619
run 4	10.0	0.050	200	36.14	0.675
run 5	10.0	0.025	400	33.45	0.818

The average turnover that can be achieved in the flow-focussing microreactor at a fixed Q_C flow rate of 2.0 mL/min is approximately 8 g of polymer particles per hour. However, as the pressure drop in the microreactor is quite low under these flow conditions, experiments were extended to flow rates up to 10.0 mL/min. Table 3 summarizes additional experimental runs in which NIP particles were synthesized at Q_C flow rates of 2.0, 4.0, 6.0, 8.0, and 10.0 mL/min and Q_C/Q_D flow rate ratios between 20 and 400.

When Q_C was increased from 2.0 to 4.0 mL/min a similar exponential decrease of the mean particle size was observed at higher Q_C/Q_D flow rate ratios (Figure 7). However, a further increase of the continuous phase flow rate led to a reduced control on the mean particle size caused by certain instabilities of the segmentation process. Consequently, a significant broadening of the particle size distributions was observed as clearly indicated by higher span(84/16) values (see Table 3).

We have investigated this upcoming instability of the segmented flow in the flow-focussing microreactor by an inverse microscope equipped with a high speed camera. In general, three different flow patterns could be observed while varying Q_C (Figure 8). At very low flow rates of the continuous phase ($Q_C \leq$ 0.5 mL/min) a certain pulsation of the shearing cone could

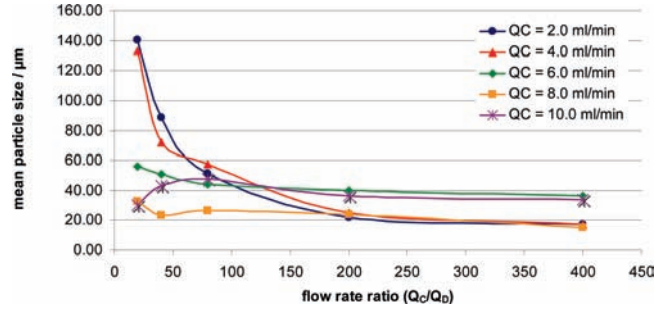

Figure 7. **Mean particle sizes of polymer beads synthesized in the flow-focussing microreactor at different flow rates of the continuous phase and different flow rate ratios.**

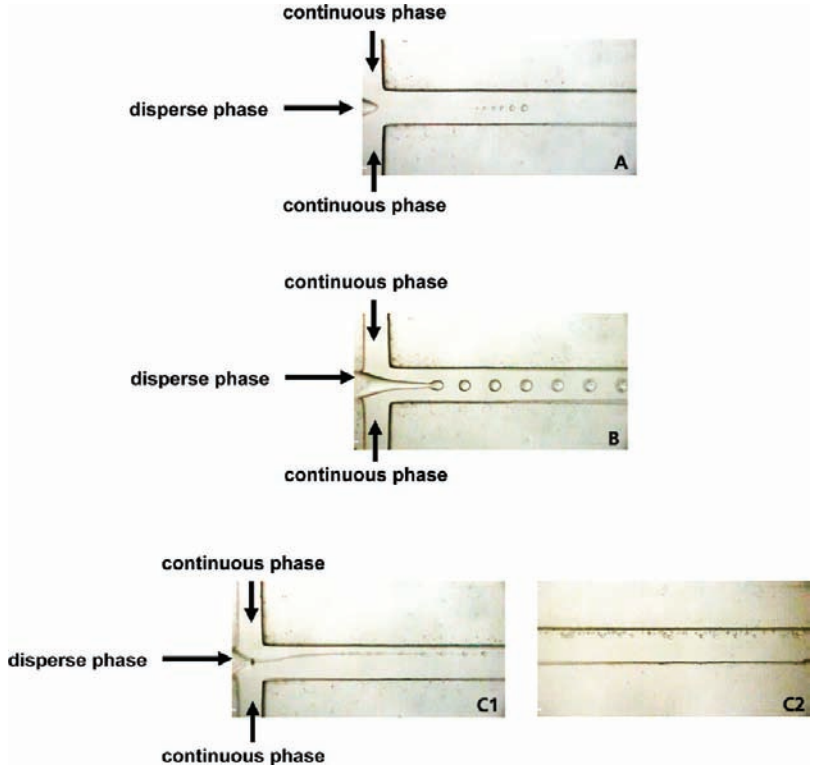

Figure 8. **Three distinct flow patterns observed in the flow-focussing microreactor at different flow rates of the continuous phase. (A) pulsation of the shearing cone at $Q_C \leq 0.5$ mL/min; (B) stable segmentation process at 0.5 mL/min $\leq Q_C \leq 4.0$ mL/min; (C) uncontrolled elongation of the disperse phase at $Q_C > 4.0$ mL/min.**

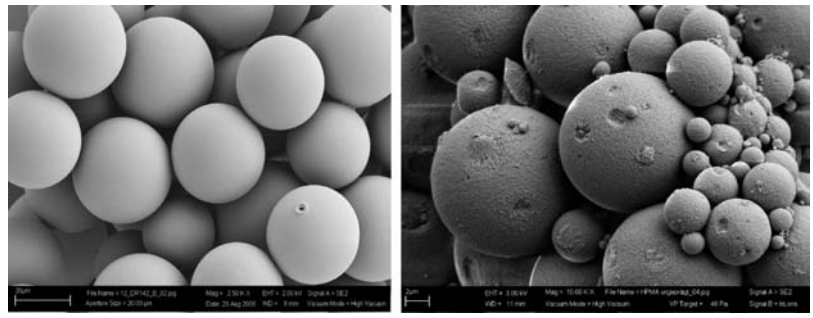

Figure 9. **Differences in texture and porosity of polymer beads. (Left) SEM image of monodisperse polymer beads with plain surfaces obtained from the T-junction microreactor process without using PEG as coporogen. (Right) SEM image of polymer beads obtained from the batch polymerization process showing strongly agglomerated but highly porous particles of different sizes.**

be observed resulting in segmented droplets of various sizes (Figure 8A). At 0.5 mL/min $\leq Q_C \leq$ 4.0 mL/min a stable segmentation process was observed forming monodisperse droplets (Figure 8B). However, at higher flow rates ($Q_C > 4.0$ mL/min) uncontrolled elongation of the disperse phase occurred, providing chaotic droplet formation and thus broad particle size distributions (Figure 8C).

Enhancing Inner Surfaces of MIP Beads. To enhance the sensing performance of MIP particles a highly functionalized inner surface is required that is accessible by the analyte (here: vaporous TNT). The MIP beads synthesized in the first series of microreactor experiments (T-junction microreactor and flow-focussing microreactor) had an inner surface of only 20−40 m^2/g which was by a factor of 10 smaller than the inner surface of MIP particles synthesized in classical batch polymerisation processes (300−400 m^2/g).

The reason for this small inner surface size and low porosity is the different curing procedures applied in the batch and microreactor processes. In the batch polymerization process curing is performed over 24 h at 60 °C using AIBN as a thermally activated radical initiator. In contrast, curing in the microreactor processes is performed more rapidly in only 30 min at room temperature using Irgacure 819 as photo initiator. Due to this tremendous reduction of curing time in the microreactor processes, chloroform (which is used as an effective porogen in the batch process) has no big impact on the generation of porous bead structures. Consequently, MIP beads with plain outer surfaces (Figure 9) and low porosity were formed.

To increase the porosity and thus enlarge the inner surface of the MIP beads we modified the formulation by employing PEG 32.000 as a coporogen. By adding a solution of 1.0 g PEG in 50 mL of chloroform to the disperse phase the inner surface of the polymer beads could be significantly enlarged to approximately 330 m^2/g (Figure 10). Higher amounts of PEG, however, led to agglomeration effects, resulting in larger particle

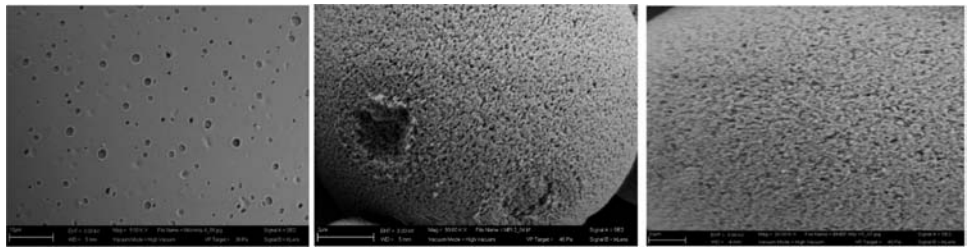

Figure 10. **SEM images of polymer bead surfaces synthesized in a flow-focussing microreactor. (Left) without using PEG as coporogen, (Middle and Right) porous inner and outer surface when PEG is used as coporogen.**

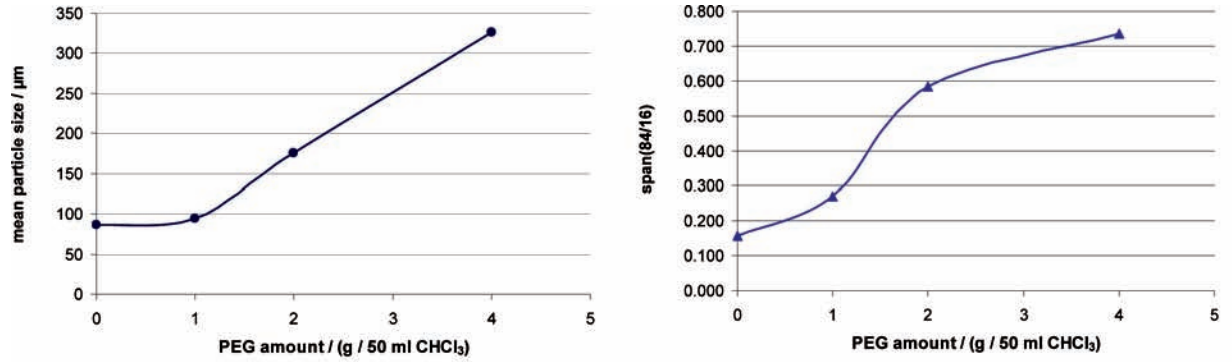

Figure 11. **Impact of increasing the PEG amount on the mean particle size and size distribution (here: polymer beads synthesized in a flow-focussing microreactor at Q_C = 2.0 mL/min and Q_D = 0.050 mL/min).**

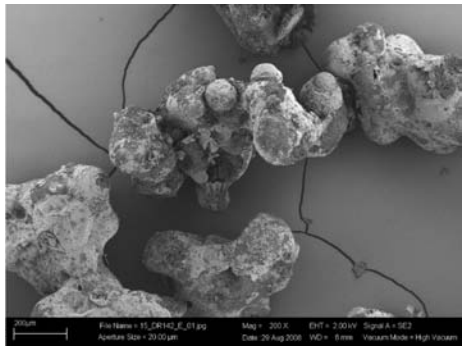

Figure 12. **SEM images of agglomerated polymer particles obtained at high PEG concentrations (4 g of PEG in 50 mL chloroform).**

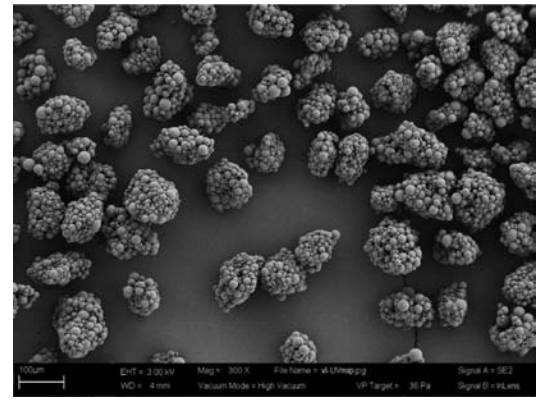

Figure 13. **SEM images of agglomerated polymer particles obtained after 30 min photocuring in batch experiments (without using porogen).**

sizes and broad size distributions. For example, increasing the PEG amount to 4.0 g in 50 mL of chloroform under constant flow conditions in a flow-focussing microreactor led to particle sizes of >300 μm and span(84/16) values of >0.700 (Figure 11). SEM pictures confirmed the agglomeration of MIP particles at higher concentrations of PEG which acts as a glue under these experimental conditions (Figure 12).

For the sake of completeness it should be mentioned that the substitution of the AIBN-based curing by a photocuring process was also investigated in small-batch experiments. After premixing of the two phases for 15 min the curing was initiated by starting the UV source. Complete curing of the polymer particles was achieved after a radiation time of 30 min. However, in contrast to the microreactor experiments the resulting polymer particles were strongly agglomerated and showed a broad mean particle size distribution (Figure 13). As no PEG was used in the experiments the inner surface was as small as in the microreactor experiments (37 g/m^2).

Conclusions

Molecularly imprinted polymer (MIP) beads based on acrylate formulations have been successfully synthesized in segmented flow processes employing microstructured reactors. Spherical polymer beads with mostly monodisperse particle size distributions have been obtained by two different methods of droplet formation, namely, shearing (in a T-junction microreactor) and constriction (in a flow-focussing microreactor). The mean particle size of the MIP beads could be adjusted in a wide range from 10 to 140 μm by deliberately changing the flow rate ratios of the continuous and the disperse phase.

By adding PEG as a coporogen to the disperse phase, MIP beads with sufficiently high porosity and large inner surface areas have been prepared as they are required for sensor applications. The MIP particles synthesized in this work have been particularly imprinted for the selective uptake of vaporous TNT. With such TNT-imprinted acrylates we have currently achieved uptake capacities of 0.2−0.3 ng TNT per mg of

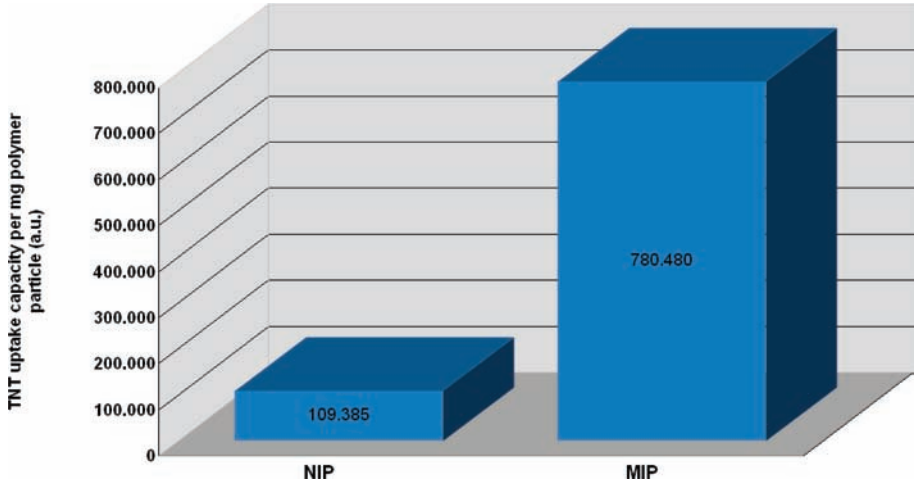

Figure 14. **Comparison of TNT vapor uptake by NIP and MIP particles (after 20 h at 70 °C).**

imprinted polymer measured by employing specially developed TNT vaporization test equipment. This equipment allows continuous gas sparging of substrates with TNT-saturated nitrogen followed by a quantitative analysis of the uptake on the basis of thermal desorption and gas chromatography (details are given in ref 24). The test equipment was also used to investigate the selective TNT uptake of MIP particles in comparison to the corresponding nonimprinted NIP particles of similar size and porosity. In Figure 14 the uptake capacities of MIP and NIP particles are compared after a 20 h exposure to TNT saturated nitrogen at 70 °C. While NIP particles show only superficial adsorption of TNT, the imprinted polymer beads exhibit a high selectivity for TNT vapor uptake.

Acknowledgment

Part of this work has been financially supported by the Landesstiftung Baden-Wuerttemberg gGmbH, Germany (Grant Number 2-4332.62-ICT/26). Skillful assistance of Bastian Horn and Eva Tissen is also gratefully acknowledged.

Received for review July 13, 2009.

OP9001774